Comparison of Wave Power Extraction by a Compact Array of Small Buoys and by a Large Buoy

X. Garnaud[1] and C.C. Mei[2]

[1]Department of Aeronautics and Astronautics,
Massachusetts Institute of Technology,
77 Massachusetts Avenue, Cambridge MA 02139
E-mail: garnaud@ladhyx.polytechnique.fr

[2]Department of Civil Engineering,
Massachusetts Institute of Technology,
77 Massachusetts Avenue, Cambridge MA 02139
E-mail: ccmei@mit.edu

Abstract

Wave Energy Converters (WEC) are usually designed to achieve maximum efficiency by impedance matching with the incoming waves. We first review the typical features of a heaving buoy. One feature is that the buoy must be large enough in order to resonate in the usual frequency range of the sea waves. Another is that the frequency range of high efficiency is band-limited, as in many other devices based on impedance matching. Inspired by the FO3 system being developed in Norway by Fred Olsen and ABB Associates, and the Manchester Bobber from UK, we examine theoretically power extraction by a compact array of small buoys. It is shown that such systems have certain advantages over a single large buoy.

Keywords: Homogenization, linear hydrodynamics, wave energy, water waves.

Nomenclature

Throughout this paper, physical variables and parameters are distinguished by asterisks, and their normalized counter parts by the same letters without the asterisks. All normalizations are defined when they first appear in the text.

x^*, y^*, z^* = dimensional coordinates.
t^* = dimensional time.
h^* = water depth.
a^*, H^* = buoy radius and draft.
d^* = separation of buoys in a square array.
L^* = total width of a strip array.
R^* = radius of a circular array.
f = area fraction covered by buoys.
x, y, z = co-ordinates normalized by h^*.
ϕ = dimensionless velocity potential.
λ_g = dimensionless coefficient of energy absorption rate.
$\mathscr{E}$ = ratio of absorbed energy to incoming energy per unit crest length .
$\mathscr{W}^*$ = capture width.
μ = small parameter = a^*/h^*.
ω = dimensionless frequency.

© Proceedings of the 8th European Wave and Tidal Energy Conference, Uppsala, Sweden, 2009

1 Introduction

From the hydrodynamic perspective, one of the simplest Wave Energy Converters is a buoy whose heaving oscillations in waves can be used to extract wave energy for electricity generation or desalination. For infinitesimal waves the basic hydrodynamic information for such devices can be obtained theoretically by existing numerical methods. In particular, for a vertical cylinder of circular cross section, the linearized problems of diffraction and radiation have been solved by [1–3], while the apparent mass and radiation damping coefficients have been calculated by [3]. Possible energy absorption has been considered by [4]. Approximate theories [5–8] have been devoted to the collective effect of many buoys under the assumption of weak mutual interactions (i.e. far from Bragg resonance [9, 10]). More comprehensive numerical methods have also been developed to study the mutual interactions in diffraction and radiation problems, without accounting for energy extraction (See e.g. [11–15]).

Three recent designs are not based on impedance matching. Each of them involves a compact array of small buoys gathered on a large platform. One is the FO3 system initiated by Fred Olsen in Norway and being developed by ABB & Associates (http://www.abb.com/). The second is the Manchester Bobber system initiated by Peter Stansby in UK (http://www.manchesterbobber.com/). In both systems the platform is a square in plan form. The Wave Star, the third system under development in Denmark, has only

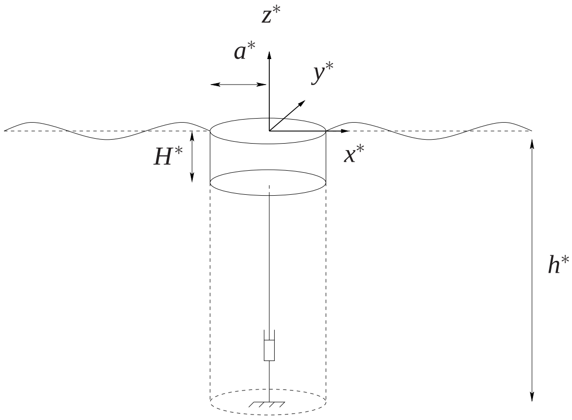

Figure 1: Sketch of the system. Energy extractor is symbolized by the dashpot.

two rows of small buoys lined along two sides of a long beam (http://www.WaveStarEnergy.com). In this article we summarize a theory relevant to both the FO3 and the Manchester Bobber.

As a gage for assessing the virtues of the compact array, wave power extraction by a single buoy is first reexamined. We then outline an approximate analysis of the interaction between an incoming wave and a compact array of small buoys. Numerical results for the two systems are compared. A fuller theory of the compact array will appear elsewhere [16].

2 Characteristic features of wave energy extraction by a single buoy.

In this section we sketch the mathematical solution and present numerical results to reveal certain key features of wave power extraction. These features are then examined analytically to facilitate physical understanding.

2.1 Non-dimensionalization

In this study, water is modeled as an inviscid and incompressible fluid. The velocity field $\boldsymbol{u}^*$ is irrotational and related to the potential ϕ^* by $\boldsymbol{u}^* = \nabla\phi^*$ where ϕ^* is Laplacian. It is well known that in the linearized framework, the mathematical theory of wave-body interaction can be decomposed into three steps [17]. We first solve the problem of scattering by fixed bodies, and then the problem of radiation by body motion of unit amplitude. Finally, the motion amplitude will be found by coupling the two problems via the dynamics of the floating buoys. The derivation of the equations governing the flow is standard, and can be found in [17].

In order to keep numerical simulation as simple as possible, we consider the buoy to be a vertical cylinder with radius a^* and draft H^*. We also assume that the water depth is constant and equal to h^*, as shown in Fig. 1. Finally, we consider a monochromatic incoming plane wave of frequency ω^* and amplitude A^*, and only look at the time harmonic response. The time factor $\exp(-\mathrm{i}\omega^* t^*)$ will be omitted.

Let us use h^* to scale distances and $\sqrt{h^*/g^*}$ to scale time, and introduce normalized variables and parameters as follows,

$$\begin{aligned} &\boldsymbol{x}^* = h^*\boldsymbol{x}, \quad t^* = t\sqrt{\frac{h^*}{g^*}}, \quad p^* = \rho^* g^* A^* p, \\ &\eta^* = A^*\eta, \quad \zeta^* = A^*\zeta, \quad \phi^* = A^*\sqrt{g^* h^*}\phi, \\ &k^* h^* = k, \quad a^* = h^* a, \quad H^* = h^* H. \end{aligned} \tag{1}$$

etc., where ρ^* is the fluid density, g^* the gravity constant, η^* the free surface elevation, ζ^* the vertical displacement of the buoy and k^* the wave number of the incoming wave.

The incoming wave is given by the following potential:

$$\phi_i^*(\boldsymbol{x}^*, t^*) = \mathrm{Re}\left\{A^* Z^*(z^*)\exp(\mathrm{i}k^* x^*)\right\} \tag{2}$$

with

$$Z^*(z^*) = \frac{g^*}{\mathrm{i}\omega^*}\frac{\cosh(k^*(z^*+h^*))}{\cosh(k^*h^*)}. \tag{3}$$

The frequency and wavenumber are related by the usual dispersion relation

$$\omega^{*2} = g^* k^* \tanh(k^* h^*) \quad \text{i.e.} \quad \omega^2 = k\tanh(k), \tag{4}$$

where

$$\omega^* = \omega\sqrt{\frac{g^*}{h^*}}. \tag{5}$$

In what follows, all quantities are dimensionless, unless otherwise specified. The symbol Re (real part of) will be omitted.

2.2 Flow and buoy displacement

Taking advantage of the cylindrical geometry, we express the incoming wave potential as [18]

$$\phi_I(\boldsymbol{x}, t) = Z(z)\sum_{m=0}^{\infty}\varepsilon_m \mathrm{i}^m J_m(kr)\cos(m\theta), \tag{6}$$

where J_m is the m^{th} Bessel function and ε_m the Jacobi symbol ($\varepsilon_0 = 1$ and $\varepsilon_n = 2\ \forall n \geq 1$). The total potential ϕ can be decomposed as the sum

$$\phi = \phi_I + \phi_S + \phi_R \tag{7}$$

of the incident wave ϕ_I, scattered ϕ_S and radiated ϕ_R wave potentials. The latter two are expanded as Fourier series

$$\phi_S = \sum_m \phi_S^{(m)}(r,z)\cos(m\theta), \quad \phi_R = \sum_m \phi_R^{(m)}(r,z)\cos(m\theta).$$

By separation of variables, the amplitude functions $\phi_S^{(m)}$ and $\phi_R^{(m)}$ can be expressed as eigenfunction function expansions both outside and under the buoys. For example for $r \geq a$, we have

$$\phi_S^{(m)} = \sum_n b_{nm}\psi_{nm}(r) f_n(z), \tag{8}$$

where the radial eigenfunctions are

$$\psi_{0,m} = H_m^{(1)}(kr), \quad \psi_{nm}(r) = K_m(k_n r) \text{ for } n \geq 1,$$

with $H_m^{(1)}$ being the Hankel functions of the first kind and K_m the Kelvin functions. The vertical eigenfunctions are

$$f_0 = \frac{\sqrt{2}\cosh(k(z+1))}{\sqrt{1+\sinh^2 k/\omega^2}}, \qquad k\tanh k = \omega^2, \tag{9}$$

$$f_n = \frac{\sqrt{2}\cos(k_n(z+1))}{\sqrt{1+\sin^2 k_n/\omega^2}}, \qquad k_n \tan k_n = -\omega^2, \tag{10}$$

where k and k_n, $n = 1,2,3,\ldots$ are respectively the real and imaginary solutions of the dimensionless dispersion relation. Note in particular that $k = k^* h^*$ is just 2π times the ratio of depth to wavelength, and increases monotonically with the frequency ω according to the dispersion relation. Under the buoy $r \leq a$, we use instead

$$\Phi_S^{(m)} = \phi_m^P + \sum_n B_{nm}\Psi_{nm}(r)F_n(z), \tag{11}$$

where the eigenfunctions are

$$\Psi_{0m} = r^m, \qquad \Psi_{nm} = I_m(\kappa_n r),\ n \geq 1, \tag{12}$$

$$F_0(z) = \frac{1}{\sqrt{1-H}}, \quad F_n(z) = \frac{\sqrt{2}\cos(\kappa_n(z+1))}{\sqrt{1-H}}, \tag{13}$$

with

$$\kappa_n = \frac{n\pi}{1-H}. \tag{14}$$

Matching the radial velocity and the pressure over the cylindrical interface $r = a$, $-1 \leq z \leq -H$ leads to algebraic equations for the expansion coefficients b_{nm} and B_{nm}, as in [1] or [3]. These can then be solved numerically.

The exciting (diffraction) force on the stationary buoy by the incident and scattered waves is, in physical variables,

$$F_z^{D*} = \mathrm{i}\rho^*\omega^* \int_0^{a^*} \Big[Z^*(-H^*)J_0(k^*r^*) + \phi_S^{(0)*}(r^*,-H^*)\Big] r^*\,\mathrm{d}r^*, \tag{15}$$

which follows by integrating Bernoulli's equation over the buoy bottom.

Note that only the isotropic mode corresponding to $m = 0$ results in a net heaving force on the buoy. Defining the normalized vertical exciting force F_z^D by

$$F_z^{D*} = \rho^* g^* h^{*2} A^* F_z^D, \tag{16}$$

then

$$F_z^D = \mathrm{i}\omega \int_0^a \Big(Z(-H)J_0(kr) + \phi_S^{(0)}(r,-H)\Big) r\,\mathrm{d}r. \tag{17}$$

Similarly, the restoring force due to the buoy motion is normalized according to:

$$F_{zz}^* = \rho^* h^{*5/2} g^{*-1/2} F_{zz},$$

and the dimensionless restoring force is

$$F_{zz} = 2\mathrm{i}\pi\omega \int_0^a \phi_R^{(0)}(r,-H) r\,\mathrm{d}r.$$

It is customary to decompose the restoring force into real and imaginary parts

$$F_{zz} = -\lambda_{zz} + \mathrm{i}\omega\mu_{zz},$$

where λ_{zz} is the heave damping coefficient and μ_{zz} the heave added mass coefficient. The total hydrodynamic force applied to the buoy is then

$$F_{hydro} = F_z^D - \mathrm{i}\omega\zeta F_{zz} + \pi a^2\zeta, \tag{18}$$

where the last term is the hydrostatic force due to buoyancy.

Let the power extraction device exert a damping force on the buoy:

$$F_{gen}^* = \mathrm{i}\omega^*\lambda_g^*\zeta^*, \tag{19}$$

where λ_g^* is the extraction rate. In dimensionless form we have

$$F_{gen} = \mathrm{i}\omega\lambda_g\zeta, \tag{20}$$

where the dimensionless extraction coefficient is defined by

$$\lambda_g = \frac{\lambda_g^*}{\rho^* g^* \pi a^{*2}}\sqrt{\frac{g^*}{h^*}}. \tag{21}$$

Applying Newton's law to the buoy gives

$$-M\omega^2\zeta = F_z^D - \omega^2\mu_{zz}\zeta - \mathrm{i}\omega\zeta(\lambda_{zz}+\lambda_g) + \pi a^2\zeta. \tag{22}$$

From (22) the buoy displacement is given by

$$\zeta = \frac{F_z^D}{\pi a^2 - \omega^2(M+\mu_{zz}) - \mathrm{i}\omega(\lambda_g+\lambda_{zz})}. \tag{23}$$

From the numerical solution of the scattering and radiation problems the dependency of the dimensionless amplitude of the buoy's displacement on the depth-to-wavelength ratio $k = k^*h^*$ is plotted in Fig. 2.

2.3 Energy extraction

The rate of energy dissipated by the linear damper – i.e. the extracted energy – is given in dimensionless form by

$$\begin{aligned}\overline{\dot{E}} &= \frac{1}{2}\lambda_g\omega^2|\zeta|^2 \qquad (24)\\ &= \frac{1}{2}\frac{\lambda_g\omega^2|F_z^D|^2}{(\pi a^2-\omega^2(M+\mu_{zz}))^2+\omega^2(\lambda_g+\lambda_{zz})^2}.\end{aligned}$$

It is related to the dimensional extracted power by

$$\overline{\dot{E}}^* = \rho^* h^{*3/2} g^{*1/2} A^{*2}\overline{\dot{E}}. \tag{25}$$

Conditions for maximum energy extraction are (i) resonance

$$\pi a^2 - \omega^2(M+\mu_{zz}) = 0, \tag{26}$$

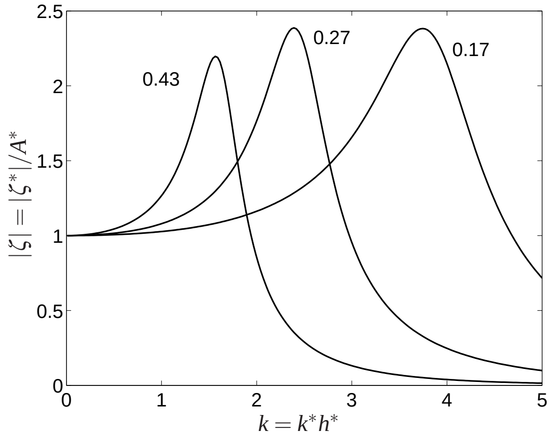

Figure 2: Normalized amplitude of the buoy displacement for three buoys. The buoy draft H is assumed to be the same as the radius a. The energy extraction rate λ_g is chosen to be a constant such that the energy extraction is maximum at resonance. Three buoys of $a = a^*/h^* = 0.17, 0.27, 0.43$ are shown.

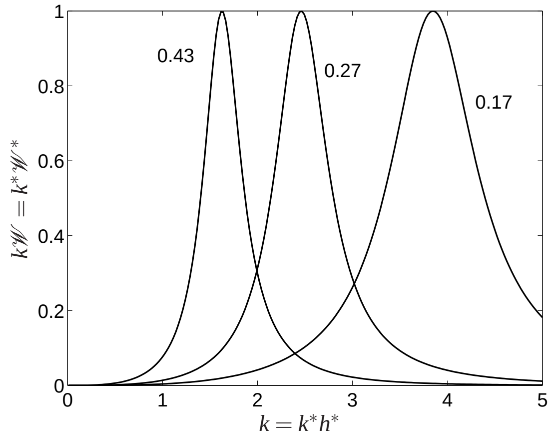

Figure 3: Energy extraction and buoy movement for three different sizes of buoys with $a = H$. The dimensionless energy extraction rate λ_g is constant and chosen such that the energy extraction is maximum at resonance, and the value of $a = a^*/h^*$ is indicated next to the curves.

and (ii) that the extraction rate equals the radiation damping rate

$$\lambda_g = \lambda_{zz}. \tag{27}$$

Therefore it is best to choose the buoy size so that the resonance frequency coincides with the peak frequency of the incoming sea spectrum. It is known analytically that the maximum power that can be extracted from a buoy with only one degree of freedom (heave) is equal to the energy influx across one wave length of the crest (See [17, §(8.9.3)]) which is, in dimensionless form:

$$\overline{\dot{E}}_{max} = \frac{C_g}{2k}, \tag{28}$$

where C_g is the group velocity of the incoming wave. We can define the capture width $\mathscr{W}$ such that the extracted energy equals the energy influx across that portion of the incident wave front. This leads to

$$\begin{aligned} k\mathscr{W} &= \frac{\overline{\dot{E}}}{\overline{\dot{E}}_{max}} \\ &= \frac{k}{C_g}\frac{\lambda_g \omega^2 |F_z^D|^2}{\omega^2(\lambda_{zz}+\lambda_g)^2 + (\pi a^2 - \omega^2 (M+\mu))^2}. \end{aligned} \tag{29}$$

Fig. 3 shows the computed dependency of the capture width with the depth-to-wavelength ratio k.

2.4 General features

To understand the numerical results better, let us now examine in more detail the characteristic features of energy extraction, and provide approximate estimates for small buoys.

2.4.1 Resonant frequency

It can be seen in Figs. 2 and 3 that as the resonant k, denoted by k_N, increases (hence the resonant wavelength decreases and the resonant frequency ω_N increases) as the size of the buoy decreases. We see in (29) that resonance occurs when the total effective inertia (due to

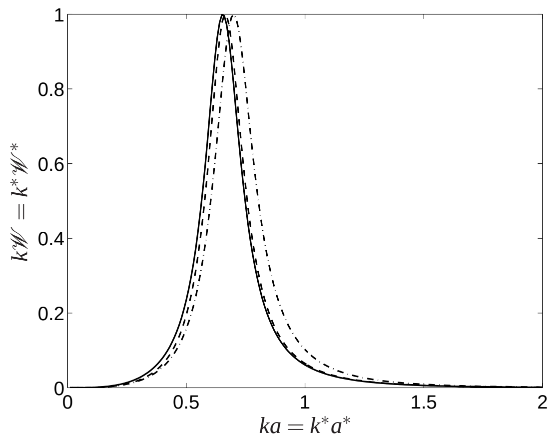

Figure 4: Capture widths for three single buoys of different radius (solid line: $a(= a^*/h^*) = 0.17$, dashed line $a(= a^*/h^*) = .27$, dash-dotted line $a(= a^*/h^*) = 0.43$.). For all buoys, $a = H$.

the physical and added mass) balances the hydrostatic buoyancy force (as all other terms are slowly varying). Strictly speaking the added mass μ_{zz} is a function of the buoy size and frequency. Assuming that it is at most of the order of the physical mass (i.e. $M + \mu_{zz} = \alpha M$ with $\alpha = O(1)$) which is proportional to a^3, and that the draft of the buoy is of the order of its radius, (26) gives

$$\omega_N^2 = O\left(\frac{1}{a}\right), \tag{30}$$

which implies

$$k_N a = O(1) \tag{31}$$

because of (4). This estimate is confirmed by numerical results shown in Fig. 4.

2.4.2 Bandwidth

Recall that at resonance, the dimensionless capture width is unity. Assuming again that F_Z^D, λ_{zz}, μ_{zz} and

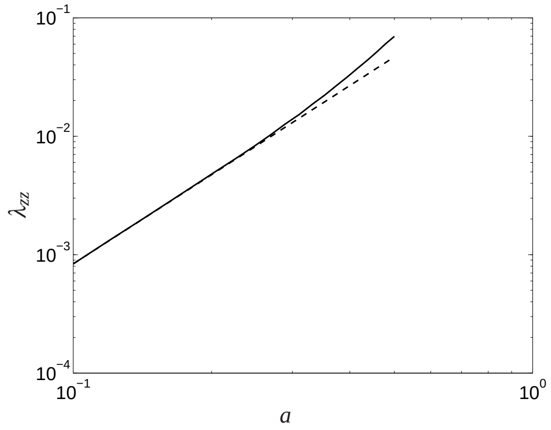

Figure 5: Radiation damping coefficient at resonance. Solid line: numerical computation. Dashed line: analytical estimate $\lambda_{zz} \propto a^{5/2}$

$\frac{k}{C_g}\omega^2$ do not have sharp variations around resonance, we can consider in a first approximation that the capture width is approximately

$$k\mathscr{W} \approx \frac{\Lambda^2}{\pi^2 a^4 (1-\alpha a\omega^2)^2 + \Lambda^2}, \tag{32}$$

where

$$\Lambda = 2\,(\lambda_{zz}\omega)|_{\omega=\omega_N}. \tag{33}$$

Estimating $k \approx \omega^2$ and solving for the values $k^{\pm}_{1/2}$ such that the capture width drops to half its maximum, i.e.,

$$k\mathscr{W}|_{k=k^{\pm}_{1/2}} = 1/2, \tag{34}$$

we get

$$k^{\pm}_{1/2} = \frac{\pm\Lambda + \pi a^2}{\alpha\pi a^3}. \tag{35}$$

The bandwidth of the resonant peak can be approximated by

$$\Delta_k = k^{+}_{1/2} - k^{-}_{1/2} = 2\frac{\Lambda}{\alpha\pi a^3}.$$

From numerical computations we find that the radiation coefficient varies with the buoy size according to

$$\lambda_{zz} = O(a^{5/2}), \tag{36}$$

as shown in Fig. 5. Using (30), we get $\Lambda = O(a^2)$ so that

$$\Delta_k = O(a^{-1}), \qquad \text{or} \qquad \Delta_k a = O(1). \tag{37}$$

Thus if $k\mathscr{W}$ is plotted against ka, the bandwidth of the capture width, remains approximately constant. This is indeed confirmed by the computed results shown in Fig. 4.

2.4.3 Heave amplitude

Recall that the capture width is given by

$$k\mathscr{W} = \frac{k}{C_g}\omega^2\lambda_g|\zeta|^2.$$

At resonance, we have just shown that $k_N = O(a^{-1})$, $\omega_N = O(a^{-1/2})$, $C_{g_N} = O(a^{1/2})$, $k_N\mathscr{W} = 1$ and $\lambda = O(a^{5/2})$. It follows that

$$|\zeta| = O(1). \tag{38}$$

This shows that the heave amplitude at resonance is independent of the size of the buoy. It is again confirmed by numerical results shown in Fig. 2. The heave velocity however increases with ω_N therefore as $a^{-1/2}$.

2.5 Summary

For convenience we summarize below the following characteristics of wave energy extraction by a single buoy:

- The maximum capture width is 1 for any buoy size.
- The frequency at which this maximum occurs satisfies the order equality $k_N a = O(1)$. Thus the wavelength is of the order of the buoys radius. In practical terms, only a large buoy with a size 1/6 of a wavelength can be resonated.
- The bandwidth increases as the size of the buoy decreases. This might suggest a potential advantage of small buoys. Note however it is impossible to have both a low resonant frequency and a wide bandwidth, without adding controlling devices of the power-takeoff system. (See e.g. [19, 20]).

3 Wave energy extraction by a compact array

As explained in the previous section, a single buoy has some limitations for energy extraction. Inspired by recent developments in Norway and UK, we now turn to the study of an array of small buoys mounted tightly on a large rig. In this section, we shall consider a square array, as shown in Fig. 6. A new length d^*, representing the separation between the centers of adjacent buoys, characterizes the array.

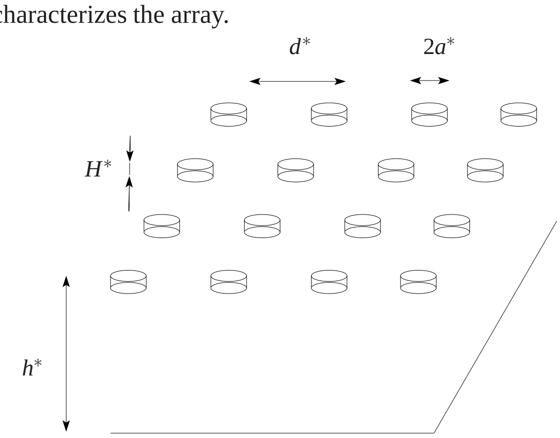

Figure 6: A compact array of small buoys

3.1 Averaged governing equations

We shall assume that the sea depth and the dimension of the rig are comparable to the incident wavelength. Then two sharply different length scales are present in the problem. First is the macro-scale given by the water depth or the wave length. Next is the micro-scale characterized by the size of the buoy which is comparable to the spacing between buoys. As in many two-scale problems, it is useful to average over the micro-scale to get the effective equation on the macro-scale. For a periodic micro-geometry, the systematic theory of homogenization, or the perturbation method of multiple scales, can be applied. Briefly, in addition to the dimensionless macro-scale coordinates defined as before: $(x^*,y^*,z^*) = h^*(x,y,z)$, we introduce the set of micro-scale coordinates, denoted by primes,

$$(x^*,y^*,z^*) = a^*(x',y',z'). \tag{39}$$

The two coordinate systems are related by

$$(x,y,z) = \mu(x',y',z'), \quad \text{where} \quad \mu \equiv \frac{a^*}{h^*} \ll 1 \tag{40}$$

is the key parameter of our study. The time scale, given by the incoming wave, is the same as in §2. We next apply the method of multiple scales to derive equations that will reflect the micro-scale geometry in a set of modified equations for the macro-scale (See e.g. [9, 10] for applications of this method to other water wave scattering problems). Details involve the solution of micro-scale boundary value problems in a unit cell. At the leading order the cell problem is homogeneous hence the potential depends only on the macro coordinates (x,y,z) but not on the micro coordinates $(x',y'z')$. At the next order the cell problem is inhomogeneous, The solvability condition leads to the effective equation and boundary conditions on the macro-scale. The derivation of the equations is presented fully in [16]; only the key results are cited here.

At the bottom of the buoy, the heave velocity must equal the water velocity. Due to the small size, the buoy inertia is relatively small and negligible. The forces on the buoy are dominated by the hydrodynamic pressure force, buoyancy restoring force and the reaction force from the extractor. From these two conditions (kinematic and dynamic) the buoy displacement can be eliminated so that one macro-scale condition is obtained for the velocity potential on the buoy-covered surface,

$$\boxed{\frac{\partial \phi}{\partial z} - \omega^2\left[1 + f(\mathscr{F}_0 - 1)\right]\phi = 0, \quad z = 0,} \tag{41}$$

where

$$f \equiv \frac{\pi a^{*2}}{d^{*2}} = \frac{\pi a^2}{d^2} \tag{42}$$

is the area fraction of solid, or the *packing ratio*, $d = d^*/h^*$ is the dimensionless spacing and

$$\mathscr{F}_0(\omega) = \frac{1}{1 - \mathrm{i}\lambda_g \omega} \tag{43}$$

expresses the effect of the energy absorber. For circular cylinders in a square array, $a^* \le d^*/2$, hence $0 < f < \frac{\pi}{4}$.

Conditions inside the fluid volume and on the seabed remain unchanged, namely

$$\nabla^2 \phi = 0, \quad -1 < z < 0, \tag{44}$$

and

$$\frac{\partial \phi}{\partial z} = 0, \quad z = -1. \tag{45}$$

Once the macro-scale variation of the velocity potential is found, the buoy displacement is given by

$$\zeta = \mathrm{i}\omega \mathscr{F}_0(\omega)\, \phi|_{z=0}\,. \tag{46}$$

For simple harmonic progressive waves the dispersion relation is complex

$$\omega^2\left(f\mathscr{F}_0(\omega) + (1-f)\right) = k\tanh(k), \tag{47}$$

thus the eigenvalues k and $k_n, n = 1,2,3,\ldots$ as well as the associated vertical eigenfunctions are also complex (see [16]).

The boundary condition (41) is the key result of the present theory[1]

It is instructive to give a more physical and heuristic derivation, as follows. Consider one small buoy. The kinematic and dynamic conditions coupling the motions of water and the buoy are, in dimensional form:

$$\frac{\partial \phi^*}{\partial z^*} = \frac{\partial \zeta^*}{\partial t^*}, \tag{48}$$

and

$$M^* \frac{\partial^2 \zeta^*}{\partial t^{*2}} = \rho^* g^* \pi a^{*2} \zeta^* - \lambda_g^* \frac{\partial \zeta^*}{\partial t^*} - \rho^* \pi a^{*2} \frac{\partial \langle \phi^* \rangle}{\partial t^*} \tag{49}$$

where λ_g^* is the dimensional extraction rate and $\langle \cdot \rangle$ denotes the spatial average over the bottom of the buoy. For small buoys both conditions can be approximately applied on the mean sea level $z^* = 0$, and as the typical scale of ϕ^* is much larger than the size of the buoy, $\langle \phi^* \rangle$ can be replaced by ϕ^* in (49). The two conditions can then be combined to one:

$$\left(M^* \frac{\partial^2}{\partial t^{*2}} + \rho^* g^* \pi a^{*2} + \lambda_g^* \frac{\partial}{\partial t^*}\right) \frac{\partial \phi^*}{\partial z^*} + \rho \pi a^{*2} \frac{\partial^2 \phi^*}{\partial t^{*2}} = 0. \tag{50}$$

For simple harmonic motion (41) becomes

$$\left(1 - \frac{M^* \omega^{*2} + \mathrm{i}\lambda_g^* \omega^*}{\rho^* g^* \pi a^{*2}}\right) \frac{\partial \phi^*}{\partial z^*} - \frac{\omega^{*2}}{g^*} \phi^* = 0. \tag{51}$$

The above condition is applied at $z^* = 0$. By Archimedis principle $M^* = \rho^* \pi a^{*2} H^*$ where H^* is the small draft.

[1] If no energy absorber is present, (41) can be used to model freely floating ice floes.

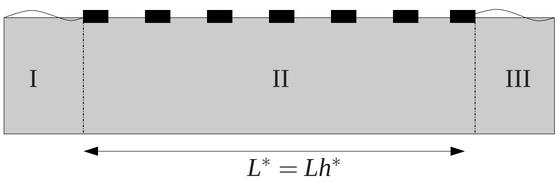

Figure 7: Cross section of an infinitely long array of finite width.

The ratio $M^*\omega^{*2}/(\rho^* g^* \pi a^{*2}) = \omega^{*2} H^*/g^* = O(\mu)$ is small, hence buoy inertia is negligible to the first order of approximation. Recalling the definition of the dimensionless extraction coefficient we rewrite (51) in dimensionless form,

$$\frac{\partial \phi}{\partial z} - \frac{\omega^2}{1 - \mathrm{i}\lambda_g \omega}\phi = 0, \quad z = 0, \tag{52}$$

under each buoy. Over the free surface not occupied by buoys the condition is well known

$$\frac{\partial \phi}{\partial z} - \omega^2 \phi = 0, \quad z = 0. \tag{53}$$

Let f be the area fraction of the free surface covered by buoys, then the averaged free surface condition is

$$(1-f)\left(\frac{\partial \phi}{\partial z} - \omega^2 \phi\right) + f\left(\frac{\partial \phi}{\partial z} - \frac{\omega^2}{1 - \mathrm{i}\lambda_g \omega}\phi\right) = 0, \tag{54}$$

which leads to (41).

Let us now present results in two cases.

3.2 Strip array

We first consider a strip array[2] of total width L as shown in Fig. 7, with its edges parallel to the crests of incoming plane waves. For simplicity, we assume the array forms an infinitely long strip in the direction of y. Imposing the continuity of mass flux and pressure at the edges of the array, we can solve analytically for the potential in and outside the array using eigenfunction expansions (as in [1] and see [21, 22] for details about the effect of (41)). Let R and T denote the reflection and transmission coefficients respectively. Then $\mathscr{E}$, the ratio of power absorption rate to the incoming power flux per unit crest length, is found by energy conservation

$$\mathscr{E} = 1 - |T|^2 - |R|^2, \tag{55}$$

which measures the efficiency of power extraction. Computed results are shown in Fig. 8. Note in Fig. 8(b) that larger L leads to a higher efficiency. Note also that the gain of $\mathscr{E}$ by using a wider array is the most important at low frequency. For a given sea spectrum at a specific site, such information can help determine the

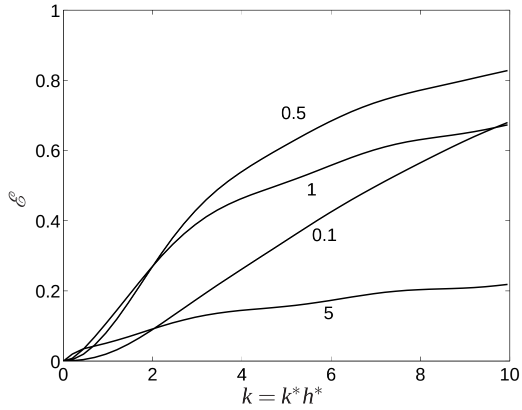

(a) Effects of extraction rate for $L = 1$.

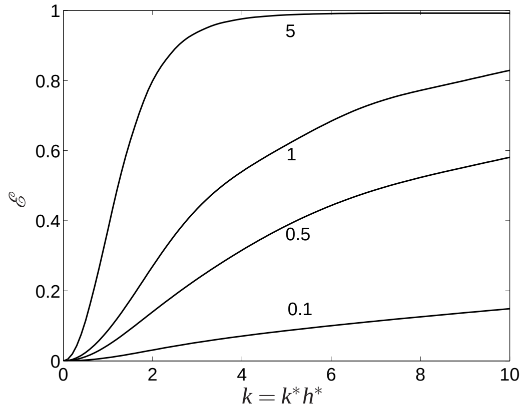

(b) Effects of total array width for $\lambda_g = 0.5$.

Figure 8: Variation of the extraction efficiency of a long array of finite width with (a) the extraction rate λ_g for a given array width and (b) the array width L for a given λ_g. Values of the varying parameter are indicated by numbers next to each curve. The packing ratio is $f = 0.2$.

optimal width of a strip-array based on efficiency and construction costs.

In general scattering is significant, hence the maximum efficiency of energy extraction is somewhat lower than that a large beam-sea device such as a Salter's duck (see [23]).

3.3 Circular array

We now consider a large number of buoys gathered inside a circle of radius R, as shown in Fig. 9. This geometry is amenable to analytical solution, unlike the square rigs in current designs of FO3 and Manchester Bobber. The problem is very similar to that of a single buoy of circular cross section, and can be treated with similar mathematical technique. Once the velocity potential is obtained, the absorbed power can be evaluated either from the far field wave amplitude or from the buoy displacement. Energy is normalized in the same way as in §2.

Sample results of the capture widths are shown in In Fig. 10 for two outer radii $R = R^*/h^*$. Similar to a large single buoy, a larger circular array yields more energy at low frequency, and there exists an optimal value for the

[2] Due to our assumptions this analysis does not apply to the Wave Star system which has only a few rows of small buoys.

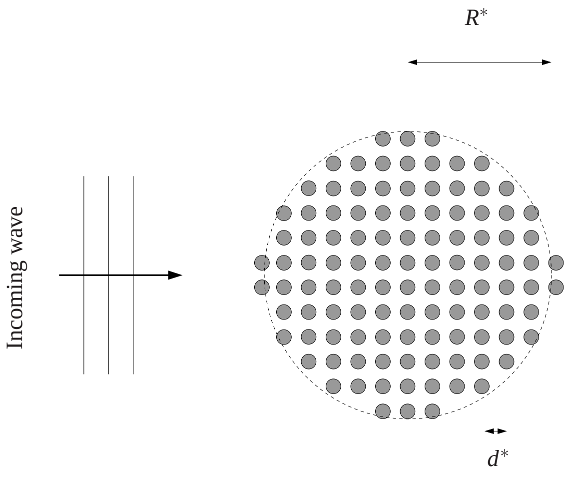

Figure 9: A circular array of energy-absorbing buoys.

damping rate. We have also examined the ratio

$$\mathscr{E} = \mathscr{W}/2R = \mathscr{W}^*/2R^* \tag{56}$$

as an alternative measure of efficiency. It is found that a circular array never absorbs more energy than what enters across a diameter of the array. Plots are omitted here.

In Fig. 11 we compare the capture widths $k\mathscr{W}$ for three circular arrays with three single buoys. The arrays have the overall radii of $R^* = (0.5, 1, 2)h^*$. The draft of each single buoy is assumed to be the same as its radius a_b^*, and is chosen so as to have the same total volume as all the small buoys in the comparison array of overall radius R^*. The draft of a small buoy is H^*. In normalized form the volume of a single buoy of radius a_b and draft a_b is πa_b^3 and the total volume of the buoys in a rig is $f\pi R^2 H$. Equating the two we get $a_b = (fR^2H)^{1/3}$. In Fig. 11 we display the capture widths for three values of $a_b = 0.17, 0, 27, 0.43$. It is clear that the compact array is hydrodynamically very promising since it can extract much more energy than a single buoy of equal volume, and with a much larger bandwidth.

The results above give theoretical confirmation of the enthusiasm expressed by the FO3 and Manchester Bobber teams.

4 Conclusion

Through simple models, we have derived the characteristic features of wave energy extraction, first for a single buoys of arbitrary size and then for a compact array made of a large number of small buoys. In the latter case, we have taken advantage of the two contrasting length scales to avoid extensive numerical work. Instead, we have proposed an asymptotic approximation and gained physical insight with minor computational effort. We have shown that gathering small point absorbers close to each other leads to an increase in the number of degrees of freedom of the device and can be advantageous. For the same amount of material much higher energy extraction over a broad frequency band can be achieved.

Additional technical challenges remain, of course. For example, can the rate of energy extraction from each

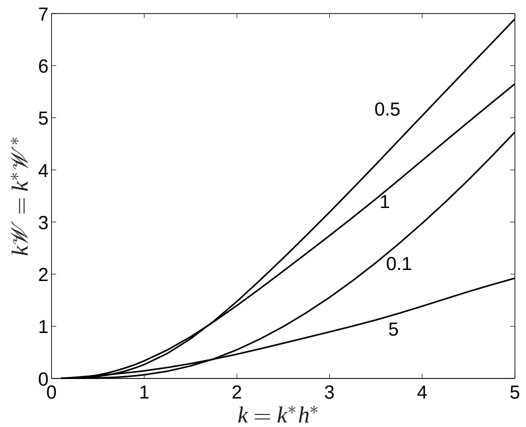

(a) $R(= R^*/h^*) = 1$

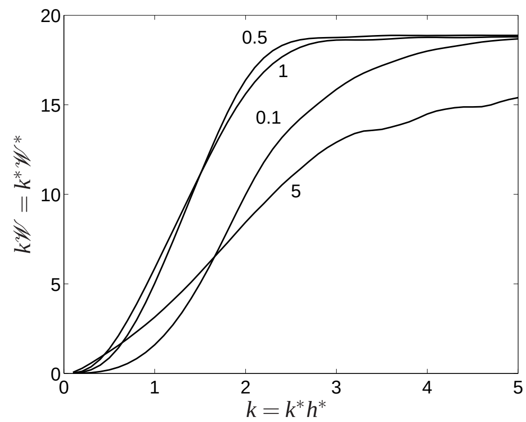

(b) $R(= R^*/h^*) = 5$

Figure 10: Dependence of capture width on the extraction rate λ_g whose values are indicated next to the curves. The packing ratio is $f = 0.2$.

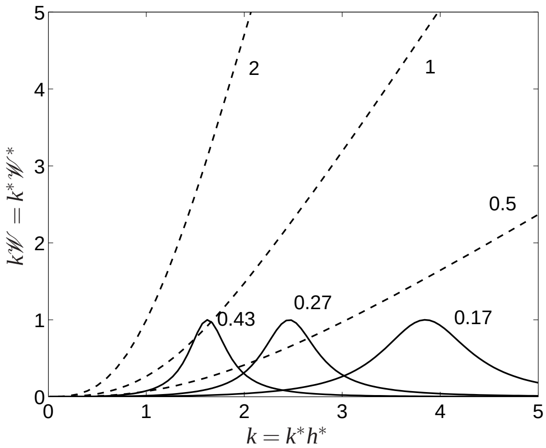

Figure 11: Capture widths of a circular arrays of small buoys of radii $R = R^*/h^* = 0.5, 1, 2$, $f = 0.2$ and $\lambda = 0.5$ are shown by dashed curves. Their dimensionless drafts are the same: $H = H^*/h^* = 1/10$. Capture width of large buoys of radii a_b and draft a_b, are shown by solid curves, for $a_b = (fR^2H/d)^{1/3} = 0.17, 0.27, 0.43$. For the single buoys the extraction rate is chosen to be the optimum at the peak.

buoy be separately controlled to increase the overall efficiency? To what extent does the platform movement influence energy extraction? What is the power potential of dozens or hundreds of these platforms in a large array? Mooring systems, nonlinear effects of finite-amplitude waves and frictional loss due to flow separation must all be considered for more comprehensive mathematical modeling of actual designs. These and the questions of cost and safety are worth further study.

Acknowledgements

We thank Drs. Yuming Liu and Dick Yue of MIT for illuminating discussions. We also thank the referees for critical comments of an earlier version and for alerting us of the Manchester Bobber and the Wave Star systems. This research has been supported by a grant from MASDAR Institute of Science and Technology in the program of MIT-Abu Dhabi Alliance. Partial support has been received from US-Israel Bi-National Science Foundation and from an ignition grant by MIT Earth System Initiative.

References

[1] J.L. Black, C.C. Mei, and M.C.G. Bray. Radiation and scattering of water waves by rigid bodies. *Journal of Fluid Mechanics*, 46(1):151–164, 1971.

[2] C.J.R. Garrett. Wave forces on a circular dock. *Journal of Fluid Mechanics*, 46(1):129–139, 1971.

[3] R.W. Yeung. Added mass and damping of a vertical cylinder in finite-depth waters. *Applied Ocean Research*, 3:119–133, 1981.

[4] K. Budal and J. Falnes. A resonant point absorber of ocean-wave power. *Nature*, 256(5517):478–479, August 1975.

[5] J. Falnes. Radiation impedance matrix and optimum power absorption for interacting oscillators in surface waves. *Applied Ocean Research*, 2(2):75–80, April 1980.

[6] J. Falnes and K. Budal. Wave-power absorption by parallel rows of interacting oscillating bodies. *Applied Ocean Research*, 4(4):194–207, 1982.

[7] J. Falnes. Wave-power absorption by an array of attenuators oscillating with unconstrained amplitudes. *Applied Ocean Research*, 6(1):16–22, 1984.

[8] A.F. de O. Falcão. Wave-power absorption by a periodic linear array of oscillating water columns. *Ocean Engineering*, 29(4):1164–1186, 2002.

[9] Y. Li and C.C. Mei. Multiple resonant scattering of water waves by a two-dimensional array of vertical cylinders: Linear aspects. *Phys. Rev. E*, 76(016302), 2007.

[10] Y. Li and C.C. Mei. Bragg scattering by a line array of small cylinders in a waveguide. part 1. linear aspects. *Journal of Fluid Mechanics*, 583(-1):161–187, 2007.

[11] C. M. Linton and D. V. Evans. The interaction of waves with arrays of vertical cylinders. *Journal of Fluid Mechanics*, 215:549–569, 1990.

[12] H. D. Manihar and J. N. Newman. Wave diffraction by a long array of cylinders. *Journal of Fluid Mechanics*, 339:309–330, 1997.

[13] C.M. Linton and R. Mclver. The scattering of water waves by an array of circular cylinders in a channel. *Journal of Engineering Mathematics*, 30(-1):661–682, 1996.

[14] P.G. Chamberlain. Water wave scattering by finite arrays of circular structures. *IMA J Appl Math*, 72(1):52–66, 2007.

[15] C.M. Linton and D.V. Evans. The radiation and scattering of surface waves by a vertical circular cylinder in a channel. *Philosophical Transactions: Physical Sciences and Engineering*, 338(1650):325–357, 1992.

[16] X. Garnaud and C.C. Mei. Wave power extraction by a compact array of buoys. *accepted for publication in Journal of Fluid Mechanics*, 2009.

[17] C.C. Mei, M. Stiassnie, and D.K.P Yue. *Theory and application of ocean surface waves.* World Scientific, 2005.

[18] M. Abramowitz and I.A. Stegun. *Handbook of mathematical functions.* Dover Publications., 1964.

[19] J. Falnes. Optimum control of oscillation of wave-energy converters. *International Journal of Offshore and Polar Engineering*, 12:147–155, 2002.

[20] A. F. de O. Falcão. Phase control through load control of oscillating-body wave energy converters with hydraulic pto system. *Ocean Engineering*, 35(3-4):358–366, March 2008.

[21] R.A. Dalrymple, M.A. Losada, and P.A. Martin. Reflection and transmission from porous structures under oblique wave attack. *Journal of Fluid Mechanics*, 224:625–644, 1991.

[22] P. McIver. The dispersion relation and eigenvalue expansion for water waves in porous structures. *Journal of Engineering Mathematics*, 34:319–334, 1998.

[23] A.E. Mynett, D.D. Serman, and C.C. Mei. Characteristics of Salter's cam for extracting energy from ocean waves. *Applied Ocean Research*, 1:13–20, 1979.